Investigating Structural Changes Induced By Nucleotide Binding to RecA Using Difference FTIR

Blaine C. Butler, Ross H. Hanchett, Helena Rafailov, and Gina MacDonald
Department of Chemistry, James Madison University, Harrisonburg, Virginia 22807 USA

ABSTRACT Nucleotide binding to RecA results in either the high-DNA affinity form (Adenosine 5′-triphosphate (ATP)-bound) or the more inactive protein conformation associated with a lower affinity for DNA (Adenosine 5′-diphosphate (ADP)-bound). Many of the key structural differences between the RecA-ATP and RecA-ADP bound forms have yet to be elucidated. We have used caged-nucleotides and difference FTIR in efforts to obtain a comprehensive understanding of the molecular changes induced by nucleotide binding to RecA. The photochemical release of nucleotides (ADP and ATP) from biologically inactive precursors was used to initiate nucleotide binding to RecA. Here we present ATP hydrolysis assays and fluorescence studies suggesting that the caged nucleotides do not interact with RecA before photochemical release. Furthermore, we now compare difference spectra obtained in H_2O and D_2O as our first attempt at identifying the origin of the vibrations influenced by nucleotide binding. The infrared data suggest that unique α-helical, β structures, and side chain rearrangements are associated with the high- and low-DNA affinity forms of RecA. Difference spectra obtained over time isolate contributions arising from perturbations in the nucleotide phosphates and have provided further information about the protein structural changes involved in nucleotide binding and the allosteric regulation of RecA.

INTRODUCTION

The *Escherichia coli* RecA protein is a multifunctional protein. RecA homologs have been found in all major kingdoms of living organisms (Brendel et al., 1997; Roca and Cox, 1997). RecA performs a DNA strand exchange reaction that is used in homologous genetic recombination and DNA repair processes (Roca and Cox, 1990). In addition, RecA acts as a co-protease in the cleavage of the repressor protein, LexA resulting in the initiation of the S.O.S. response (Roca and Cox, 1990). The formation of an active RecA-ATP-ssDNA nucleoprotein filament is required for both DNA strand exchange and LexA cleavage (Roca and Cox, 1997). At low salt concentrations RecA is a DNA-dependent ATPase. However, increasing salt concentrations stimulate RecA-dependent ATP hydrolysis in the absence of DNA (Pugh and Cox, 1988).

RecA exists in numerous forms consisting of oligomers, helical filaments or filamentous bundles that are dependent on the solution conditions, concentration of RecA, and the presence of cofactors including nucleotides and/or DNA (Roca and Cox, 1997; Brenner et al., 1988, 1990; Budzynski et al., 1996; Egelman, 1993). The binding of nucleotides by RecA has been characterized by at least two different DNA binding states. When RecA binds the nucleotide Adenosine 5′-triphosphate (ATP), the protein adopts an active conformation that is associated with a higher affinity for DNA. However, the binding of Adenosine 5′-diphosphate (ADP) results in an inactive RecA conformation that is marked by a lower affinity for DNA (Menetski and Kowalczykowski, 1985; Kowalczykowski and Krupp, 1995; Rehrauer and Kowalczykowski, 1993; Roca and Cox, 1990; Egelman, 1993). Thus, nucleotide binding to RecA results in the allosteric regulation of the protein. In addition to local changes around the nucleotide-binding site, the conformational changes induced by nucleotide binding are also reflected in the pitch of the protein helix and the oligomeric structure of the nucleoprotein filament (Egelman, 1993; Yu and Egelman, 1992). When RecA binds ATP or Adenosine 5′-[γ-thio]triphosphate (ATPγS), the protein filament is elongated resulting in approximately a 95-Å pitch of the protein helix (Ellouze et al., 1995; Egelman, 1993; Yu and Egelman, 1992). However, the RecA protein helix has a 60–83 Å pitch in the absence of nucleotide or when ADP is bound (Egelman, 1993; Roca and Cox, 1997; Story et al. 1992; Ellouze et al., 1995). Small angle neutron scattering studies have provided evidence that the RecA filament is elongated upon binding of either ADP or ATP, where a more extended filament is observed in the presence of ATP (Ellouze et al., 1995). Interestingly, in the presence of high salt, cofactor binding results in an even greater elongation of the RecA filament (Ellouze et al., 1995).

The three-dimensional structures of RecA in the absence of cofactor and in the presence of ADP have been determined by x-ray crystallography (Story et al., 1992; Story and Steitz, 1992). Currently, there is no crystal structure of the ATP- or DNA-bound forms of RecA. Structural information involving RecA-DNA complexes has been gathered using techniques such as fluorescence, electron microscopy, small angle neutron scattering, and circular dichroism of the complexes in solution (Takahashi et al., 1996; Roca and Cox, 1997). Previous structural and mutagenesis studies have provided information on the amino acid residues that may be involved in the allosteric regulation of RecA. Amino acids that may be perturbed upon nucleotide binding reside

Submitted May 23, 2001, and accepted for publication December 28, 2001.

Address reprint requests to Dr. Gina MacDonald, Department of Chemistry, James Madison University, Harrisonburg, VA 22807. Tel.: 540-568-6852; Fax: 540-568-7938; E-mail: macdongx@jmu.edu.

0006-3495/02/04/2198/13 $2.00

in the nucleotide-binding site, in the L2 region of the protein, at the monomer-monomer interface, and in the MAW motif. Many of these amino acids have also been implicated in regulating the function of RecA (Kelley and Knight, 1997; Roca and Cox, 1997; Egelman, 1993; DeZutter et al., 2001).

Some interesting amino acid residues in close proximity to the nucleotide-binding site are Gln194, Asp100, Tyr103, Tyr264, and Arg196 (Roca and Cox, 1997; Story and Steitz, 1992; Voloshin et al., 2000). Site-directed mutagenesis studies have implicated Asp100 in nucleotide specificity and Lys72 in ATP hydrolysis (Stole and Bryant, 1996; Shan et al., 1996; Rehrauer and Kowalczykowski, 1993). Fluorescence studies suggest Tyr264 and Tyr103 interact with both ATP and ADP (Morimatsu et al., 1995). Fluorescence studies have also implied that His163 has stronger interaction with ATP as compared with ADP (Stole and Bryant, 1994).

Interestingly, it has also been suggested that Gln194, which protrudes into the nucleotide-binding site, is involved in mediating the allosteric regulation induced by ATP binding to RecA (Story and Steitz, 1992; Kelley and Knight, 1997). Recently, it has been demonstrated that an unstructured L2-derived peptide undergoes a transition to a β-structure in the presence of ATP (Voloshin et al., 2000). Current mutagenesis studies have shown that amino acids Gln194 and Arg196, located in loop L2, the proposed DNA binding site, are involved in the allosteric regulation of RecA and are required for RecA activity (Hortnagel et al., 1999). The results of these studies suggest that Gln194 and Arg196 play significant roles in the activation of RecA, presumably forming favorable interactions with the phosphates of ATP (Hortnagel et al., 1999). In addition to amino acids located around the nucleotide-binding site, other amino acids located near the monomer-monomer interface have been implicated in the transmission of allosteric information throughout the protein. For example, Phe217, Lys6, and Arg28 have been shown to affect the oligomeric structure of the RecA filament (DeZutter et al., 2001; Eldin et al., 2000). Previous research has provided many insights into RecA function, yet questions remain about the role of specific structures and residues involved in nucleotide binding and strand exchange. The complete description of the molecular changes induced by nucleotide binding to RecA has yet to be elucidated. Therefore, important questions remain concerning the role of ATP binding and hydrolysis. To characterize all of the protein components associated with the nucleotide binding to RecA, it is essential to use a technique that will provide information about changes that occur throughout the entire RecA protein.

Fourier transform infrared (FTIR) difference spectroscopy has the potential to yield important insights into how nucleotide binding affects the entire RecA protein. This technique provides a means to study nucleotide binding to the wild-type protein and allows us to compare our results with those obtained on site-directed mutants and the L2 peptide. Previous studies in a variety of systems have shown that using the photochemical release of nucleotides from their caged complexes in conjunction with difference FTIR provides a useful tool for the investigation of nucleotide binding to a variety of proteins. This technique has provided information on the structural perturbations in both the protein and the nucleotide that are induced upon binding (Barth et al., 1990; Du et al., 2000; Cepus et al., 1998a; vonGermar et al., 1999; Raimbault et al., 1997). The use of caged nucleotides is essential for difference FTIR studies and provides the means necessary to obtain high signal-to-noise data that are generated by using a single protein sample and an external perturbation to trigger the reaction of interest. Therefore, we have used spectrophotometric activity assays and fluorescence experiments to investigate whether the presence of caged nucleotides interferes with ATP hydrolysis or the formation of the elongated ATPγS-RecA-DNA filament. Thus far, we have found no evidence that would suggest that the presence of caged nucleotides interferes with the hydrolysis of ATP or RecA binding to double-stranded DNA (dsDNA) in the presence of ATPγS and ethidium bromide. Here we begin the process of identifying the vibrations arising from crucial amino acids and structural elements of RecA that are affected by nucleotide binding. We present RecA-nucleotide minus RecA difference spectra obtained in H_2O and D_2O. Upon comparison of the RecA-nucleotide data obtained in H_2O and D_2O, we observe numerous changes that provide further evidence for unique secondary structural changes and key amino acid side chains that are involved in regulating the affinity of RecA for DNA. We also identify unique vibrations only associated with the high-DNA affinity, RecA-ATP structure. In addition, time-dependent studies allow us to follow nucleotide binding over time in the absence of any subtraction artifacts. The time-dependent spectra reveal interesting vibrations that may be associated with continued nucleotide binding and/or hydrolysis.

MATERIALS AND METHODS

RecA was obtained from Roche (Gipf-Oberfrick, Switzerland) or MBI Fermentas (Hanover, MD) and then exchanged into buffer *M* that contained 1 mM $MgCl_2$, 1 mM dithiothreitol (DTT), 0.1 mM EDTA, and 20 mM Hepes (Sigma, St. Louis, MO), pH 7.5, in either nanopure water or deuterium oxide from Isotech (Miamisburg, OH). Exchange into the appropriate buffer was performed using Centricon YM-30s (Millipore, Bedford, MA) and multiple dilution and concentration steps. Myoglobin (Sigma) was dissolved in buffer *M*. Poly(dT) was purchased from Amersham Pharmacia Biotech (Piscataway, NJ) and ATP was purchased from Sigma. The caged nucleotides, NPE-ATP and NPE-ADP (P^3-(1-(2-nitrophenyl-)ethyl)adenosine 5′triphosphate (or diphosphate, caged ADP) were purchased from Molecular Probes (Eugene, OR). Lactate dehydrogenase, pyruvate kinase, and reduced nicotinamide adenine dinucleotide (NADH) were purchased from Roche. The concentration of RecA in the two buffers was determined using the molar $\epsilon_{280} = 2.17 \times 10^4$ (Wittung et al., 1995). This molar extinction coefficient was used for RecA in both H_2O and D_2O. The caged nucleotides were dissolved in H_2O or D_2O buffer *M*.

ATP hydrolysis assays

ATP hydrolysis was monitored using an enzyme-coupled spectrophotometric assay similar to that described by Mikawa et al. (1998) with minor modifications. All assays were monitored using a Perkin-Elmer Lambda 7 (Beaconsfield, Buckinghamshire, UK) at 37°C. All ATP activity assays were performed over a range of ATP concentrations from 0.25 mM to 1.33 mM in the following buffer containing 20 mM Tris HCl, 1 mM DTT, 0.1 mM EDTA, 3.0 mM phosphoenol pyruvate, 1.0 mM $MgCl_2$, 0.32 mM NADH, and 25 units/ml of pyruvate kinase and lactate dehydrogenase at pH 7.5. The concentrations of poly(dT) and RecA were 10 μM and 1 μM, respectively. The concentration of ATPγS was 10 μM, whereas the caged nucleotide concentrations were 0.5 mM. The rates of ATP hydrolysis were calculated using $-A_{340}$ per second and the $\epsilon_{340} = 6.22\ mM^{-1}\ cm^{-1}$ for NADH (Mikawa et al., 1998). Some additional assays were performed in the absence of DNA (37°C) with the same concentration of phosphenol pyruvate, NADH, pyruvate kinase, and lactate dehydrogenase. However, these assays were performed in either 100× Hepes buffer *M* or 100× buffer *I* that was used in previous infrared experiments (Brewer et al., 2000).

Fluorescence experiments

Fluorescence experiments were performed as described (Kim et al., 1993). Calf thymus DNA, type I, was obtained from Sigma. All fluorescence measurements were performed in a buffer containing 10 mM $MgCl_2$, 1 mM DTT, 2.0 μM ethidium bromide, 25 mM sodium 2-(morpholino)ethane sulfonic acid, pH = 6.2. A FluoroMax fluorometer (SPEX, Edison, NJ) was used to follow the ethidium bromide displacement reaction. Excitation at 535 nm was used and the emission at 600 nm was followed using 1-s time increments and 1-s integration times (Kim et al., 1993). All experiments were conducted at room temperature. The RecA and nucleotides used were described previously and final concentrations were as follows: 22 μM DNA (in base pairs), 200 μM ATPγS, 4 μM RecA. In some cases caged nucleotides (200 μM) or ADP (200 or 500 μM) were added to the reaction mixture.

Infrared studies

The absorbance of amide I ($\sim$1654 cm^{-1}) for the RecA protein samples ranged from 0.21 to 0.39 absorbance units (a.u.). The RecA infrared samples contained $\sim$6–10 nmol of protein and 160–180 nmol of caged nucleotide. To mimic conditions used to generate the RecA difference spectra, the myoglobin data shown in Fig. 3 were obtained on myoglobin samples under identical conditions. These myoglobin samples had similar amide I intensities and nucleotide-to-protein ratios as those used in the RecA experiments. The Hepes buffer *M* was used for all infrared experiments presented here. Each infrared sample was prepared as described previously except for the addition of DTT to a final concentration of 10 mM in the infrared samples (Brewer et al., 2000). Infrared spectra were recorded using a 560 Magna spectrometer (Nicolet, Madison, WI) that was equipped with a Mercury cadmium telluride/A detector, cooled by liquid nitrogen. The resolution of the spectra was 4 cm^{-1}. 500 scans were co-added for each interferogram with the use of a mirror velocity of 1.8988 cm/s and a Happ-Genzel apodization function. The samples were maintained at -8 to -10°C using a Fischer Scientific water bath (Pittsburgh, PA) and a Harrick temperature controller (Ossining, NY). A nitrogen laser, 337 nm, was used to release the nucleotide from its caged complex. Difference infrared spectra were obtained by making a ratio of a single beam spectrum recorded after photolysis of the sample to one recorded before photolysis. In each of the spectra shown in Fig. 4 there was at least a 15 to 1 ratio of nucleotide to protein after photolytic release. RecA-nucleotide minus RecA difference spectra were rendered by subtracting the difference spectrum obtained in the absence of protein from a difference spectrum obtained in the presence of protein. The strong 1525 and 1346 cm^{-1} vibrations assigned to the asymmetric and symmetric NO_2 stretching vibrations were used to normalize the amount of nucleotide released in the two samples (Cepus et al., 1998b). This process allowed the isolation of vibrations associated with nucleotide binding to RecA. The amide I intensity was used to normalize the protein content between samples to generate the double difference data shown in Fig. 5. The time-dependent data were obtained by taking a spectrum immediately after the release of caged nucleotide and then ratioing subsequent scans obtained over time to the scan obtained immediately after the release (Fig. 6). Therefore, the data presented in Fig. 7 do not contain any contributions because of the photolysis of the caged nucleotide.

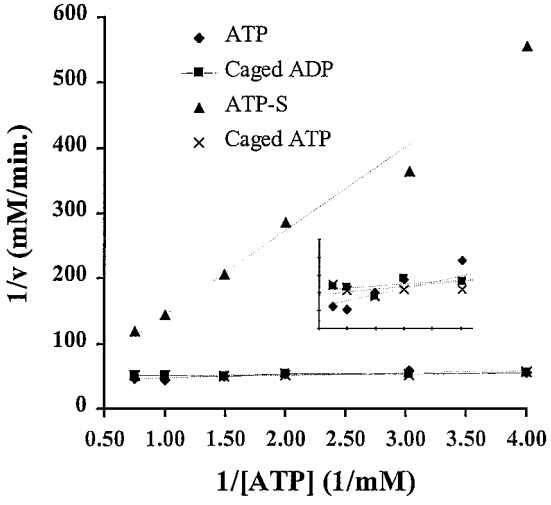

FIGURE 1 Lineweaver-Burke plots of hydrolysis assays carried out at 37°C using a NADH coupled assay to monitor ATP hydrolysis at 340 nm (Mikawa et al., 1998). Assay components were added in the following order: lactate dehydrogenase (25 u/ml), pyruvate kinase (25 u/ml), poly (dT) (10 μM), NADH (0.32 mM), ATP (0.25–1.33 mM), ATPγS (10 μM), RecA (1 μM). The symbols correspond to data obtained in the presence of ATP (◆), with ATP and 0.5 mM caged-ADP (■), with ATP and 0.5 mM caged-ATP (×), and with ATP and 10 μMATPγS (▲). The inset shows an expanded view of the same data.

RESULTS AND DISCUSSION

ATP hydrolysis and fluorescence data

ATP hydrolysis assays were monitored to determine whether the presence of caged nucleotides interfered with the ability of the RecA to hydrolyze ATP. The results of these assays were plotted as a Lineweaver-Burke plot and are shown in Fig. 1. The only nucleotide found to competitively inhibit ATP hydrolysis was ATPγS. Fig. 1 shows that the addition of 10 μM ATPγS resulted in significant reduction in RecA-mediated ATP hydrolysis. This result is consistent with previous studies that have shown that both ADP and ATPγS inhibit ATP hydrolysis by RecA (Lee and Cox, 1990). However, Fig. 1 also shows that the addition of caged ATP or caged ADP does not affect the ability of RecA to hydrolyze ATP because the rates obtained in the presence of caged nucleotides are nearly identical to those

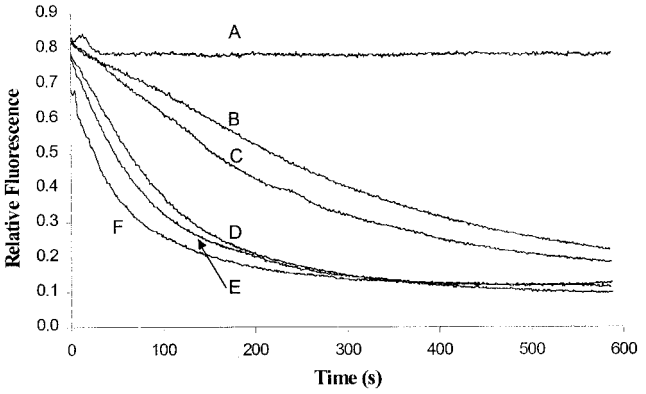

FIGURE 2 Fluorescence assays of ethidium bromide displacement by RecA (Kim et al., 1993). Reaction was carried out in a buffer containing 25 mM MES, 10 mM $MgCl_2$, 1 mM DTT, 2.0 μM Et-Br, 22 μM (base pairs) dsDNA, 4 μM RecA, pH 6.2. Nucleotide additions were as follows: (*A*), 200 μM caged ATP; (*B*), 500 μM ADP and 200 μM ATPγS; (*C*), 200 μM ADP and 200 μM ATPγS; (*D*), 200 μM caged ADP and 200 μM ATPγS; (*E*), 200 μM caged ATP and 200 μM ATPγS; and (*F*), 200 μM ATPγS.

obtained in their absence (Fig. 1). These results suggest that the caged nucleotides do not compete with ATP for the RecA nucleotide binding site. It should be noted that caged ATP is not hydrolyzed by RecA (data not shown).

ATP hydrolysis assays were also measured under conditions that mimic the buffer and ion concentrations present in the infrared samples. Recent experiments in our laboratory suggest that our infrared samples contained ~100 times the original concentration of buffer and salts after dehydration. To discern whether previous conditions using Tris buffer (Brewer et al., 2000) or current conditions that use Hepes buffer could result in ATP hydrolysis in the absence of DNA, activity assays were performed in 100 times the concentration of the two infrared buffers. The activity assays revealed that in the presence of 100× Tris buffer *I* (no DNA) only negligible ATPase activity is obtained when compared with the standard reaction conditions in the presence of polydT. However, activity assays performed in the presence of 100× Hepes buffer *M* (no DNA) used in these experiments result in substantially higher amounts of activity than obtained under standard reaction conditions in the absence of DNA. The recent assays and previous studies performed by Ellouze et al. (1995) imply that the protein may adopt a more extended conformation (especially after nucleotide binding) than present in our previous data.(Brewer et al., 2000) Furthermore, the possibility exists that our current infrared samples may be able to hydrolyze ATP in the absence of DNA.

Fig. 2 shows fluorescence experiments performed to monitor RecA-DNA interactions in the presence of caged nucleotides. Previous studies have shown that only an active RecA conformation with ATPγS bound resulted in ethidium bromide displacement from dsDNA (Kim et al., 1993). This displacement is most likely the result of elongated DNA and the intercalation of aromatic amino acids of RecA between the DNA bases (Kim et al., 1993). The binding of ADP results in an inactive RecA conformation and no ethidium bromide displacement from dsDNA. Fig. 2 shows that when RecA and ATPγS are present, the fluorescence decreases over time because of ethidium bromide displacement from the DNA.(Fig. 2 *F*) When equimolar amounts of caged compounds and ATPγS are added to the RecA-DNA solution, similar ethidium bromide displacement is observed (Fig. 2, *D* and *E*) when compared with that obtained in the absence of caged nucleotides (Fig. 2 *F*). When only caged ATP (Fig. 2 *A*) or caged ADP (data not shown) is added to the RecA-DNA solution, no ethidium bromide displacement is observed. However, when ADP and ATPγS are present in equimolar amounts, ethidium bromide displacement is decreased (Fig. 2 *C*). Furthermore, increased amounts of ADP result in further decreases in ethidium bromide displacement (Fig. 2 *B*). The later result suggests that increased amounts of competing nucleotide results in decreased amounts of RecA that are able to adopt the active more extended conformation responsible for ethidium bromide displacement. A control involving addition of equimolar amounts of polyethylene glycol with a molecular weight similar to the caged nucleotides (data not shown) resembles the data presented (Fig. 2, *D* and *E*). The results in Fig. 2 suggest that the presence of caged nucleotides does not affect formation of the active ATPγS-RecA-dsDNA filaments. If the presence of caged nucleotides interfered with the formation of the elongated protein filament and/or DNA binding, we would expect to observe decreased ethidium bromide displacement similar to that obtained in the presence of ADP. Thus, it is unlikely that the caged-nucleotides interact with the nucleotide or DNA binding sites on RecA. This new information is crucial for the interpretation of the infrared data obtained using caged nucleotides. The ATP hydrolysis assays and the fluorescence results suggest that we can assume minimal interactions between RecA and the caged nucleotides before photolysis.

Infrared difference spectra

Conformational rearrangements induced in RecA by the binding of nucleotides are of interest because of the structural and functional implications associated with the allosteric regulation of RecA. To isolate nucleotide-induced protein changes, the photolytic release of ADP and ATP from caged substrates was used in conjunction with FTIR spectroscopy. The technique used to generate RecA-nucleotide minus RecA difference spectra can be summarized using Fig. 3. Fig. 3 *A* represents a difference spectrum obtained on a sample containing RecA and caged ADP, whereas Fig. 3 *B* represents a difference spectrum obtained on a sample containing only caged ADP under identical buffer conditions. Both spectra (Fig. 3, *A* and *B*) contain vibrations because of the photolysis of the caged ADP

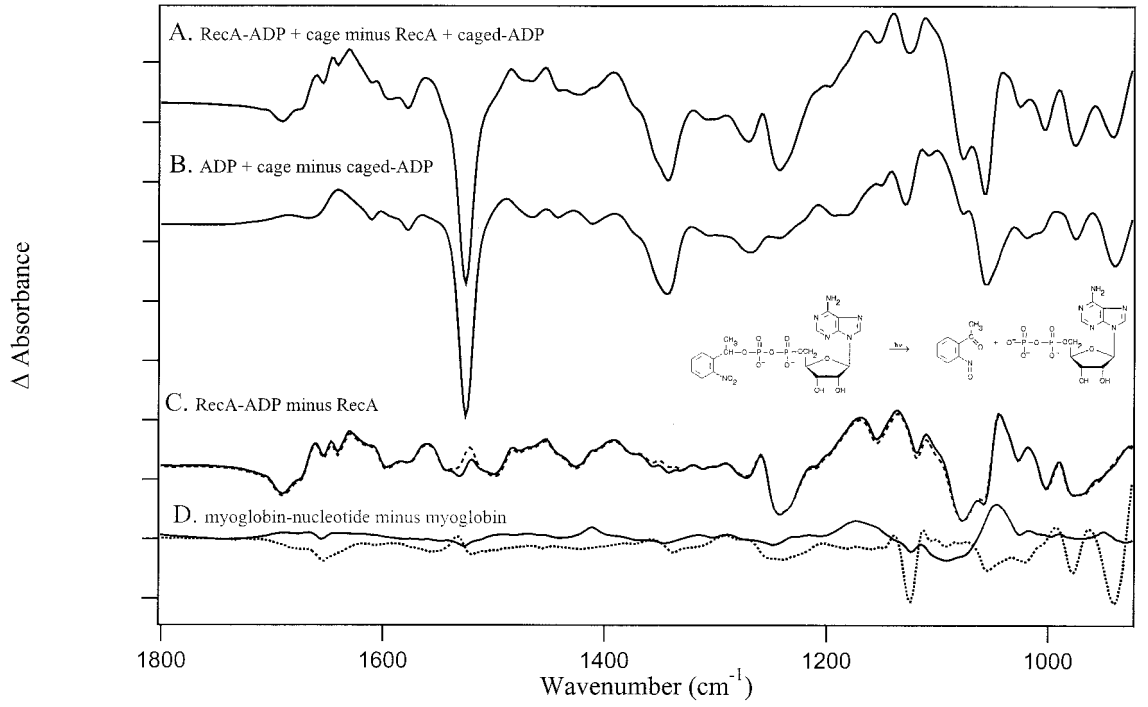

FIGURE 3 Difference FTIR spectra taken on samples containing (*A*) RecA and caged ADP, (*B*) caged ADP. Fig. 3 *C* (*solid line*) represents the RecA-ADP minus RecA + caged-ADP difference spectrum generated by normalizing the spectrum in (*B*) and then subtracting it from the spectrum shown in (*A*). The dotted line in *C* represents a separate difference spectrum obtained using a slightly different normalization factor. (*D*) Difference spectra associated with myoglobin-ADP minus ADP (*solid line*) and myoglobin-ATP minus ATP (*dotted line*). The inset shows the light-induced release of ADP from its caged substrate. The tick marks on the *y* axis correspond to 5×10^{-3} absorbance units.

(*inset*, Fig. 3). Under conditions previously used in our laboratory we have generated similar spectra to those presented in Fig. 3 (Brewer et al., 2000). However, in our previous data the photolysis of the caged-nucleotides resulted in a strong positive vibration around 1690 cm^{-1} that arises from the formation of a C = O on the free cage (Brewer et al., 2000; Barth et al., 1991; Cepus et al., 1998b). This vibration is not present in the spectra shown in Fig. 3 because of the addition of DTT in our present samples (Cepus et al., 1998b). The intense negative signal around 1525 cm^{-1} vibration is assigned to the asymmetric stretching vibration of the NO_2 and is used to normalize the contributions from the photolytic release of the cage between samples (Cepus et al., 1998b; Barth et al., 1991). The normalized caged-ADP spectrum (Fig. 3 *B*) is then subtracted from the RecA and caged-ADP spectrum (Fig. 3 *A*), resulting in the difference spectrum shown in Fig. 3 *C*. The final difference spectrum (Fig. 3 *C*) includes any changes in the protein and/or nucleotide that are induced by binding. The dotted line in Fig. 3 *C* shows an independent subtraction using the same data and a slightly different normalization factor. Comparison of the solid and dotted lines in Fig. 3 *C* shows that there is some difference in intensity around the 1520 cm^{-1} region that is not reflected in the intensity and line-shapes of the other vibrations throughout the spectrum. Fig. 3 *D* shows difference spectra associated with myoglobin-nucleotide minus myoglobin under identical conditions used to generate the spectra shown in Fig. 3 *C*. The spectra shown in Fig. 3 *D* were obtained by subtracting the caged-nucleotide spectrum from the myoglobin-nucleotide spectrum in the identical fashion used to generate Fig. 3 *C*. Fig. 3 *D* shows myoglobin-ATP minus ATP (*dotted line*) and myoglobin-ADP minus ADP (*solid line*). The difference data obtained in the presence of myoglobin reveal minimal changes around 1650 and 1630 cm^{-1} as previously observed in our laboratory (Brewer et al., 2000). However, the myoglobin-nucleotide data show more substantial differences in the 1300–900 cm^{-1} region of the spectra. As myoglobin is not known to have a nucleotide binding site, these vibrations represent the changes associated with nonspecific binding and/or artifacts attributable to the subtraction procedure used to generate the difference spectra shown in Fig. 3 *C* and Fig. 4. The vibrations below 1300 cm^{-1} in the myoglobin data suggest that similar contributions may be present in the RecA data. von Germar et al. (2000) has also suggested that below 1300 cm^{-1} there may be artificial bands because of the subtraction procedure. Therefore, when investigating the initial nucleotide binding to RecA by subtracting contributions from the photolysis reaction, we will focus on vibrations in the 1800–1300 cm^{-1} region.

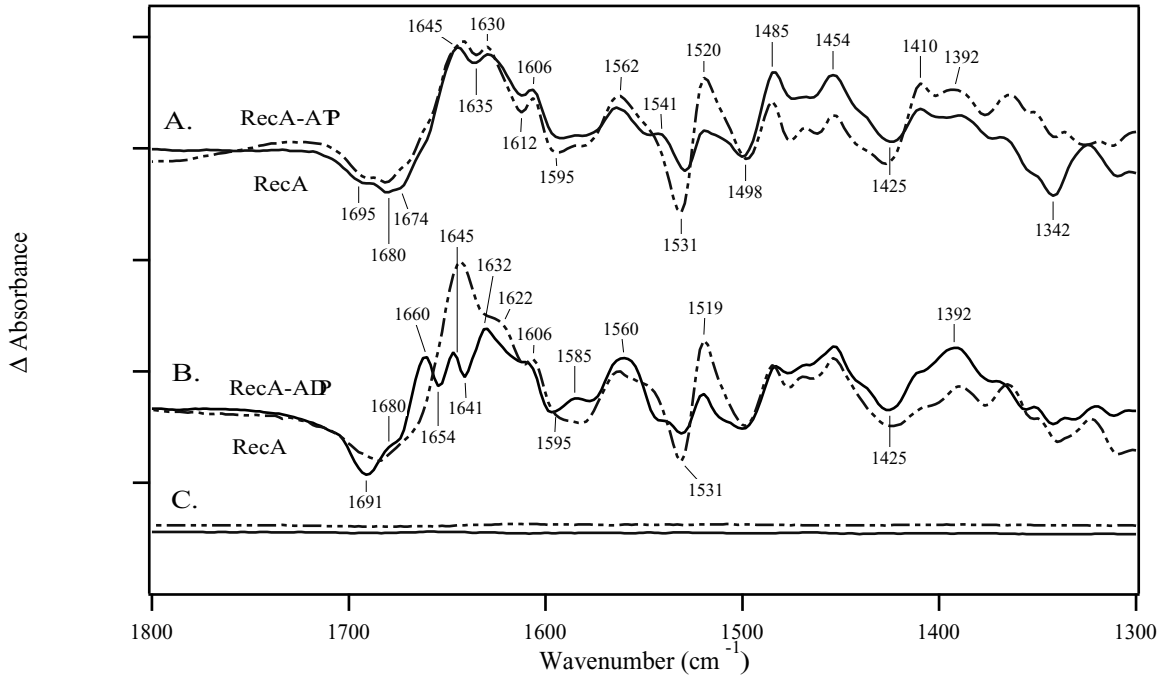

FIGURE 4 The difference spectra presented were generated by subtracting difference spectra obtained in the absence of protein, from difference spectra obtained in the presence of protein. To compare samples the amide I peak was used to normalize for protein content between samples. (*A*) RecA-ATP minus RecA difference spectra obtained in H_2O (*solid line*), and D_2O (*dotted line*). (*B*) RecA-ADP minus RecA difference spectra obtained in H_2O (*solid line*), and D_2O (*dotted line*). (*C*) Ratio of two spectra taken before photolysis on the same samples that were used to generate the spectra shown in *B* (H_2O sample, *solid line* and D_2O sample, *dotted line*). The tick marks on the *y* axis correspond to 4×10^{-3} absorbance units.

Fig. 4 *A* (*solid line*) shows a RecA-ATP difference spectra obtained in H_2O whereas Fig. 4 *B* (*solid line*) represents the RecA-ADP spectrum obtained in H_2O. These spectra are in substantial agreement with those observed in our previous work, even though the previously published spectra were obtained on RecA from a different source and taken under different buffer conditions (Brewer et al., 2000). The ADP-binding spectra show similar positive vibrations around 1660, 1645, 1632, 1606, 1560, 1519, and 1392 cm^{-1} and common negative vibrations around 1691, 1654, 1641, and 1595 cm^{-1}. However, differences are observed in the 1530 cm^{-1} region that may be ascribed to subtraction artifacts (Fig. 3 *D*). Furthermore, the present RecA-ADP data contain more intense signals throughout the spectrum, as well as a broader differential signal in the 1390–1425 cm^{-1} region than previously observed (Brewer et al., 2000). The current data (RecA-ADP and Rec-ATP) have increased signal-to-noise and we observe the appearance of additional vibrations that are most likely attributable to the enhanced initial release of the nucleotide and increased signal-to-noise ratio. Upon comparison of the current RecA-ATP with the previously obtained data, we see common positive vibrations around 1645, 1630, 1606, and 1520 cm^{-1} and common negative vibrations around 1674, 1635, and 1425 cm^{-1}. Some differences are observed in the ATP data around 1690, 1660, 1530, and 1400 cm^{-1}. In particular, a new positive vibration is observed around 1410 cm^{-1} in the present data. Differences between current and previous data that are observed around 1690 and 1530 cm^{-1} may be attributable to the subtraction artifacts. The addition of DTT in the present samples eliminates the strong positive vibration at 1690 cm^{-1} that was previously associated with the photochemical release of the nucleotide (Brewer et al., 2000). The small differences around 1530 cm^{-1} are observed in the myoglobin data (Fig. 3 *D*) and may arise from subtraction artifacts.

The RecA-ADP and RecA-ATP spectra shown in Fig. 4 contain a broad positive contribution in the 1600–1670 cm^{-1} region and broad negative contributions around 1670–1700 cm^{-1} not previously observed (Brewer et al., 2000). The broad vibrations may result from the initial binding of the nucleotide causing some reorganization of the nucleoprotein filament. When activity assays were obtained under conditions that mimic infrared sample conditions, we observe some ATP hydrolysis in the absence of DNA as described above. Therefore, we believe it is possible that nucleotide binding under present conditions may result in a more extended conformation of the filament that is able to hydrolyze ATP (Ellouze et al., 1995). Another possibility could be that the RecA filaments exist in more heterogeneous structures than were present under previous conditions (Brewer et al., 2000). Any assembly or disassembly of the nucleoprotein filament induced by nucleotide binding may also contribute to the broad features between

1600–1700 cm^{-1}. However, almost all vibrations present in the data presented in Fig. 4 are in agreement with previously published spectra (Brewer et al., 2000). Furthermore, recent difference infrared experiments performed on ADP binding to RecA in the presence of 3.6 M KCl result in unique difference spectra that reveal numerous changes (data not shown) when compared with those obtained in Fig. 4 *B* (*solid line*). The infrared changes observed in Fig. 4 reveal that we are able to detect changes that are only ~1% of the total protein absorbance (as estimated from the total amide I intensity). The extent of structural changes associated with nucleotide binding to RecA are consistent with previous studies on nucleotide binding to other proteins such as Ca^{2+}-ATPase and GroEL (Barth et al., 1991, 1990; von Germar et al., 1999).

The positive bands in the difference spectra shown in Fig. 4 represent vibrations associated with the RecA-nucleotide bound state, whereas the negative bands correspond to protein vibrations that are no longer present upon nucleotide binding. The ATP hydrolysis assays and the fluorescence results suggest that the negative contributions in these spectra arise from specific changes in RecA or nucleotide, but are not the result of any caged nucleotide-RecA interactions. To begin to identify the origin of the vibrations present in our data we have performed identical experiments in D_2O. The amide I vibrations in the absorbance spectra were used to normalize the protein content between samples. This normalization allows us to compare intensities between samples, assuming the amount of nucleotide binding in our samples is similar. We estimate that the nucleotide to protein ratio is approximately 15–20 to 1 in the data shown in Fig. 4. Comparison of the amide II vibrations in H_2O and D_2O absorbance spectra (data not shown) allows us to estimate the amount of deuterium exchange achieved in the samples used to generate the difference spectra shown in Fig. 4 (*dotted lines*). Upon comparison of the H_2O and D_2O absorbance spectra we observe a decrease amide II vibration in the 1550 cm^{-1} region (N-H) and increase in the 1450 cm^{-1} vibration (N-D) after deuterium exchange. The decrease in amide II upon exchange suggests that we obtained ~50% deuterium exchange in the samples used to generate the spectra observed in Fig. 4 (*dotted lines*) (Byler and Susi, 1986). The remaining N-H groups may be buried in the protein's hydrophobic core or not easily exchanged (Jackson and Mantsch, 1995).

Secondary structural changes

Binding of nucleotides leads to changes in the secondary structure of RecA. These changes are best observed in the intense signals present between 1700 and 1500 cm^{-1}. The amide I modes (1690–1620 cm^{-1}) are predominately attributable to the C = O groups of the peptide backbone, and are expected to shift only 5–10 cm^{-1} in D_2O (Jackson and Mantsch, 1995; Byler and Susi, 1986). The amide II vibration is composed mainly of protein backbone C-N and N-H vibrations that absorb ~1550 cm^{-1} in H_2O and shift to ~1450 cm^{-1} in D_2O (Byler and Susi, 1986). This shift opens up the 1550 cm^{-1} region of the spectra for analysis of amino acid side chains, such as Tyr and Glu, whose vibrations may have been overshadowed by the strong amide II absorbance in H_2O. Fig. 4 (*solid lines*) shows that the amide I region is affected differently by the binding of ATP and ADP in H_2O. The spectra presented in Fig. 4 do not show the sharp differential signals observed for nucleotide binding to Ca^{2+}-ATPase (von Germar et al., 2000, 1999). The observed broadening of the vibrations may arise from inhomogeneity of the nucleoprotein filaments or some reorganization of the filamentous structure, as previously discussed. However, the spectra presented in Fig. 4 are representative of those obtained on numerous samples under identical conditions.

Comparing the difference spectra obtained in H_2O and D_2O (Fig. 4, *A* and *B*) we observe a few distinct shifts, but the most noticeable changes occur in peak shapes and intensities upon deuterium exchange. Both RecA-ATP and RecA-ADP difference spectra show vibrations associated with changes in β-sheet structures (1625–1640 cm^{-1} and 1675–1695 cm^{-1} in H_2O) as well as random coil structures (1640–1648 cm^{-1}) (Jackson and Mantsch, 1995). However, the RecA-ADP spectrum has unique differential signals in the 1648–1660 cm^{-1} region (H_2O) that may be associated with changes in α-helical structures (Jackson and Mantsch, 1995; Venyaminov and Kalnin, 1990a). The RecA-ATP spectrum in H_2O (Fig. 4 *A*, *solid line*) also contains some positive contributions in the 1650–1655 cm^{-1} region. However, the ATP spectrum lacks the distinct negative vibration observed around 1654 cm^{-1} in the RecA-ADP spectrum. Therefore, ATP binding may also result in unique changes associated with α-helical structures (Jackson and Mantsch, 1995; Venyaminov and Kalnin, 1990a). As expected, all of the tentative assignments to structural changes in the amide I region show minimal downshifts in D_2O (Jackson and Mantsch, 1995; Byler and Susi, 1986). However, when comparing the H_2O and D_2O spectra of either the RecA-ADP or RecA-ATP difference data we observe increased intensity in the differential signal around 1525 cm^{-1} in D_2O. This may be attributable to amide II or amino acid side chain vibrations that shift out of this region. We do observe differences in the intensity of the 1460 cm^{-1} region when H_2O and D_2O spectra are compared. We would not expect to see the same intensity in the 1460 cm^{-1} region as observed in the 1550 cm^{-1} region in the H_2O because ~50% exchange was achieved in these samples.

Amino acid side chains

In addition to information about secondary structural changes, the difference spectra presented should also include changes in the environments of single amino acid side

chains that are affected by nucleotide binding. We would expect to see changes in Asp, Glu, Gln, Lys, Arg, Asn, His, and Tyr side chains because of previous structural and mutagenesis studies (Takahashi et al., 1996; Stole and Bryant, 1996; Kelley and Knight, 1997; Story and Steitz, 1992; Stole and Bryant, 1994; Roca and Cox, 1997; Hortnagel et al., 1999). Our results are consistent with the assumption that nucleotide binding results in perturbations of the environment around these side chains. In Fig. 4, both the ATP and ADP spectra show strong vibrations around 1520 cm^{-1} that are seen to shift slightly in D_2O. The tyrosine ring modes are known to absorb in this region in H_2O (1518 cm^{-1}) and shift only slightly upon deuterium exchange (1515 cm^{-1}) (Venyaminov and Kalnin, 1990b; Chirgadze et al., 1975; Dollinger et al., 1986). Therefore, we suggest that part of the broad differential signals observed in this region may arise from the tyrosine residues in the nucleotide binding site and/or other tyrosine residues influenced by nucleotide binding (Story and Steitz, 1992). Unfortunately, this region can also experience subtraction artifacts because of the photolytic release of the cage (Fig. 3 *C*). However, analysis of multiple difference spectra generated under identical conditions reveals consistent intensity increases in the 1520 cm^{-1} region in D_2O, leading us to believe these peaks are reproducibly enhanced in D_2O. Also present in both ATP and ADP spectra are positive contributions in the 1530–1540 cm^{-1} region in H_2O that are not present in D_2O. The positive vibration around 1535 cm^{-1} observed in H_2O could arise from a Lys side chain or a change in amide II vibration, as both are expected to have substantial downshifts in D_2O (Venyaminov and Kalnin, 1990b; Byler and Susi, 1986; Chirgadze et al., 1975). However, subtraction artifacts may also contribute to this region (Fig. 3 *C*).

Other side chains of interest include Gln (1670 cm^{-1}), Arg (1673 cm^{-1}), Asn (1678 cm^{-1}), and Lys (1629 cm^{-1} and 1526 cm^{-1}). Gln and Arg side chains show substantial shifts to ~1635 cm^{-1} and 1608 cm^{-1}, respectively, in D_2O and Asn shifts to ~1648 cm^{-1} (Venyaminov and Kalnin, 1990b; Chirgadze et al., 1975). A negative contribution that is present in the RecA-ATP H_2O spectrum (Fig. 4 *A*, *solid line*) but not observed in the RecA-ADP difference spectrum (Fig. 4 *B*, *solid line*) appears ~1674 cm^{-1} in H_2O, whereas new negative intensity is observed ~1612 cm^{-1} in the D_2O RecA-ATP spectrum. This vibration could arise from an Arg side chain. However, Gln and Asn also absorb in the 1670–1680 cm^{-1} region, and their respective shifts in D_2O may be overshadowed by other changes in the 1635–1650 cm^{-1} region. The RecA-ADP spectrum shows a positive shoulder around 1680 cm^{-1} that is not present in the RecA-ATP spectrum. It is possible that this vibration could arise from a Gln, Arg, or Asn residue that interacts differently with ADP and ATP, as this shoulder is not as prevalent in the RecA-ADP spectrum obtained in D_2O. However, unique secondary structural changes or nucleotide vibrations could also account for differences in this region (El-Mahdaoui and Tajmir-Riahi, 1995; Jackson and Mantsch, 1995; Venyaminov and Kalnin, 1990a).

The deprotonated, asymmetric stretching vibrations of Asp and Glu absorb at 1574 cm^{-1} and 1560 cm^{-1}, respectively (Venyaminov and Kalnin, 1990b). The symmetric stretching vibrations of these deprotonated groups absorb at 1402 cm^{-1} and 1404 cm^{-1} for Asp and Glu, respectively (Venyaminov and Kalnin, 1990b). The asymmetric Asp and Glu vibrations shift to ~1584 and ~1567 cm^{-1} in D_2O and are concomitant with increased absorption in D_2O (Venyaminov and Kalnin, 1990b; Chirgadze et al., 1975). We observe vibrational changes in the 1560–1580 cm^{-1} and 1400 cm^{-1} regions in both the RecA-ADP and RecA-ATP difference spectra. These changes may arise from multiple Asp and Glu side chains, as these vibrations are present in the H_2O spectra (Fig. 4, *A* and *B*, *solid lines*) and show intensity and lineshape differences upon D_2O exchange (Fig. 4, *A* and *B*, dotted lines). Again, it is important to note that nucleotide changes may also contribute to this region (El-Mahdaoui and Tajmir-Riahi, 1995). One of the most notable differences in the RecA-ADP H_2O difference spectrum is the disappearance of a positive signal around 1585 cm^{-1} upon D_2O exchange. Histidine ring vibrations are usually observed around 1596 cm^{-1} and only have very weak intensity in D_2O (Venyaminov and Kalnin, 1990b; Chirgadze et al., 1975). The weak D_2O-histidine vibration could explain why we do not observe any obvious new positive intensity in the RecA-ADP, D_2O spectrum. A second possibility for the disappearance of this vibration in the D_2O spectrum could arise from a negative arginine vibration (1633 cm^{-1} in H_2O) that shifts to ~1586 cm^{-1} and cancels the positive vibration at 1585 cm^{-1} (Chirgadze et al., 1975). In summary, there are many interesting and complex spectral features in the data presented in Fig. 4. The predicted changes resulting from nucleotide interactions with amino acid side chains such as His, Asp, Glu, Gln, Tyr, Lys, and Arg, are consistent with our data. However, vibrations arising from the nucleotide perturbations also absorb throughout this region, making definitive assignments even more difficult (El-Mahdaoui and Tajmir-Riahi, 1995; Barth et al., 1990). The D_2O data provide further support for the involvement of these side chains and other changes in secondary structural components associated with nucleotide binding, yet we are not yet able to unambiguously identify the origin of the vibrations present in the difference spectra.

Differences between ATP and ADP binding to RecA

Many changes induced by ATP or ADP binding are similar in frequency and intensity. Small overall structural changes resulted in common vibrations associated with either nucleotide binding. To try and isolate important differences between the ATP- and ADP-bound state of RecA, we used

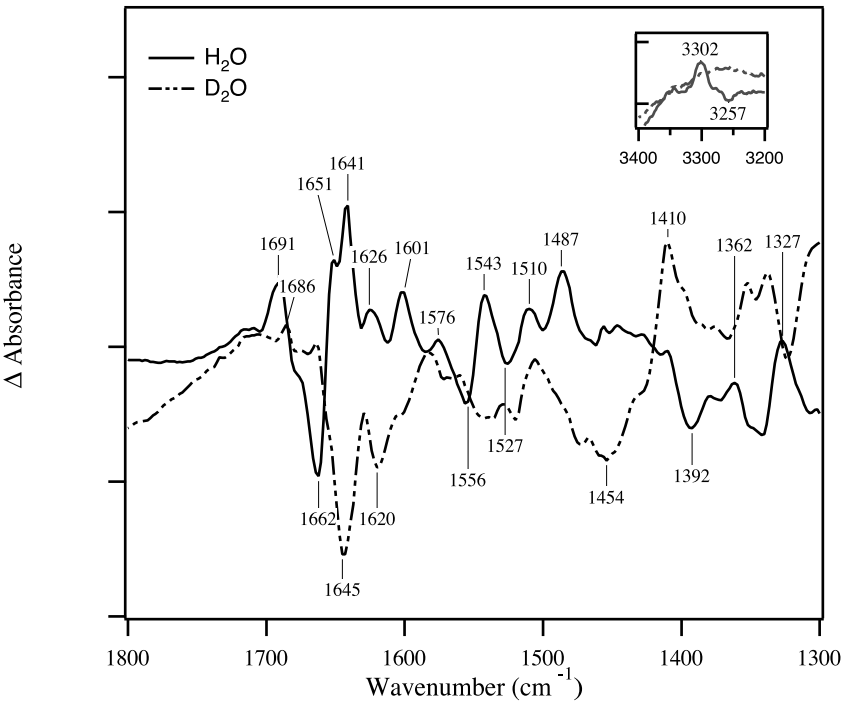

FIGURE 5 Double difference spectra were generated from the same samples used in Fig. 4 to isolate the differences between ATP and ADP binding to RecA. The solid line represents the spectrum obtained by subtracting the spectrum in 4 *B* (*solid line*) from the spectrum in 4 *A* (*solid line*) after using the amide I intensity to normalize for protein content between samples. The dotted line represents the spectrum obtained by subtracting the spectrum in 4 *B* (*dotted line*) from the spectrum in 4 *A* (*dotted line*) again using the amide I intensity to normalize for protein content between samples. The inset shows the 3300 cm^{-1} region of the same subtractions (H_2O, *solid line* and D_2O, *dotted line*). The tick marks on the *y* axis correspond to 2×10^{-3} absorbance units.

amide I intensities to normalize the protein content between samples and subtracted the RecA-ADP difference spectrum (Fig. 4 *B*) from RecA-ATP difference spectrum (Fig. 4 *A*). Fig. 5 shows double difference data that reflect RecA-ATP minus RecA-ADP spectra in H_2O (*solid line*) and D_2O (*dotted line*). It should be noted that using the amide II′ intensity to normalize protein content between samples results in a double difference spectrum very similar to the data presented in Fig. 5 (*dotted line*). The spectra in Fig. 5 should reflect *only* those vibrations that differ between ATP and ADP binding to RecA. Comparison of the data presented in Fig. 5 (*solid line*) with that previously published shows similar positive vibrations around 1691, 1651, 1626, 1543, and 1510 cm^{-1}, and a common negative vibration around 1527 cm^{-1}. The present data obtained in H_2O show additional or enhanced positive features around 1641, 1601, 1487, and 1327 cm^{-1}. The current data also show additional or enhanced negative vibrations around 1662 and 1392 cm^{-1} that may be visualized by the increased signal-to-noise ratio or differences that result from the different buffer conditions used to obtain the data as discussed previously.

The comparison of the H_2O and D_2O double-difference data reveal numerous differences as observed throughout the 1800–1300 cm^{-1} region. These differences are reflected in the shifts and cancellations throughout the spectrum. Unique alterations in secondary structures must be associated with each form of RecA. The negative amide II vibration around 1556 cm^{-1} in H_2O disappears in the D_2O spectrum and new negative intensity is observed around 1454 cm^{-1}, suggesting that this vibration arises from the peptide backbone (Byler and Susi, 1986). Other vibrations that may arise from secondary structures include the peak at 1691 cm^{-1} that shifts to ~1686 cm^{-1} in D_2O. This vibration could represent a unique β structure associated with the RecA-ATP complex. The peak at 1626 cm^{-1} in H_2O is also consistent with increased β structure in the ATP-bound state, whereas the 1651 cm^{-1} vibration would suggest unique α-helical structures in the RecA-ATP state (Jackson and Mantsch, 1995; Venyaminov and Kalnin, 1990a). De Zutter and Knight have suggested that the affinity of RecA for DNA is increased as a result of an ATP-mediated increase in filament assembly so that residues at the subunit interface, such as helices A and G, may play important roles in allosteric regulation (DeZutter et al., 2001; Takahashi et al., 1996). Experiments performed on an L2 peptide have suggested ATP binding to RecA may cause the L2 region to adopt increased β-sheet structure (Voloshin et al., 2000). The changes observed in Fig. 5 provide evidence that unique α-helical and β-sheet structures are associated with the high-DNA affinity form of RecA; other alterations in secondary structure are induced by ADP binding. In general, deuterium exchange results in more shifts as observed in Fig. 5 compared with Fig. 4. Therefore, we speculate that many of the amino acid side chains that are responsible for regulating DNA affinity and protein-protein interactions are side chains or nucleotide vibrations that are affected by D_2O exchange. The inset in Fig. 5 shows the 3300 cm^{-1} region of the same double difference spectra in H_2O (*solid line*) and D_2O (*dotted line*). His, Lys, Gln, Asn, and Arg have all been implicated in mediating the allosteric regulation of RecA (Voloshin et al., 2000; Hortnagel et al., 1999; Shan et al., 1996; Kelley and Knight, 1997; Stole and Bryant, 1994).

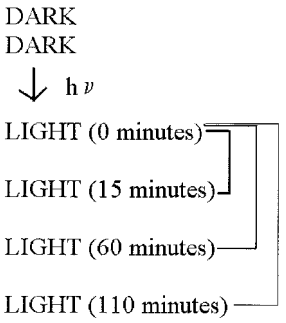

FIGURE 6 Data acquisition scheme used to generate the difference spectra presented in Fig. 7. The ratio of spectra denoted light 2, 3, or 4 versus the light 1 spectrum result in difference spectra associated with changes that occur after the photolytic release of nucleotide.

The inset provides further evidence that supports the involvement of a nitrogen-containing amino acid side chain that differs between the ATP- and ADP-bound RecA states. Hydrogen bonded N-H vibrations absorb at ~3300–3500 cm^{-1} and are expected to shift upon deuterium exchange (Bellamy, 1980; Kim et al., 1997). Although we observe vibrations around 3257 and 3302 cm^{-1} that disappear upon deuterium exchange, we do not observe new vibrations in the 2600–2400 cm^{-1} region but instead observe a very weak broad differential signal (not shown). Therefore, we will have to rely on future studies to definitively assign these vibrations to an N-H containing amino acid side chain.

Time-dependent infrared changes

The low water content and temperatures that were used to obtain the high signal-to-noise difference data presented would also be expected to slow the binding of the released nucleotides. These slow reactions have allowed us to follow some binding induced and/or hydrolysis changes over time. Fig. 6 shows a schematic of the data acquisition procedure used to generate the spectra shown in Fig. 7. To generate the spectra in Fig. 4, we ratio the first light taken immediately after photolysis to the dark spectrum obtained before photolysis. Thus, the resulting difference data in Fig. 4 may contain some artifacts, especially in the 1300–900 cm^{-1} region (Fig. 3 *D*). To eliminate any subtraction artifacts, we have taken advantage of the slow reactions present in our samples by constructing a ratio of the light spectra denoted light 2, 3, or 4 versus the original light 1 spectrum taken immediately after photolysis. This method does not require subtracting contributions from the photolysis of the caged

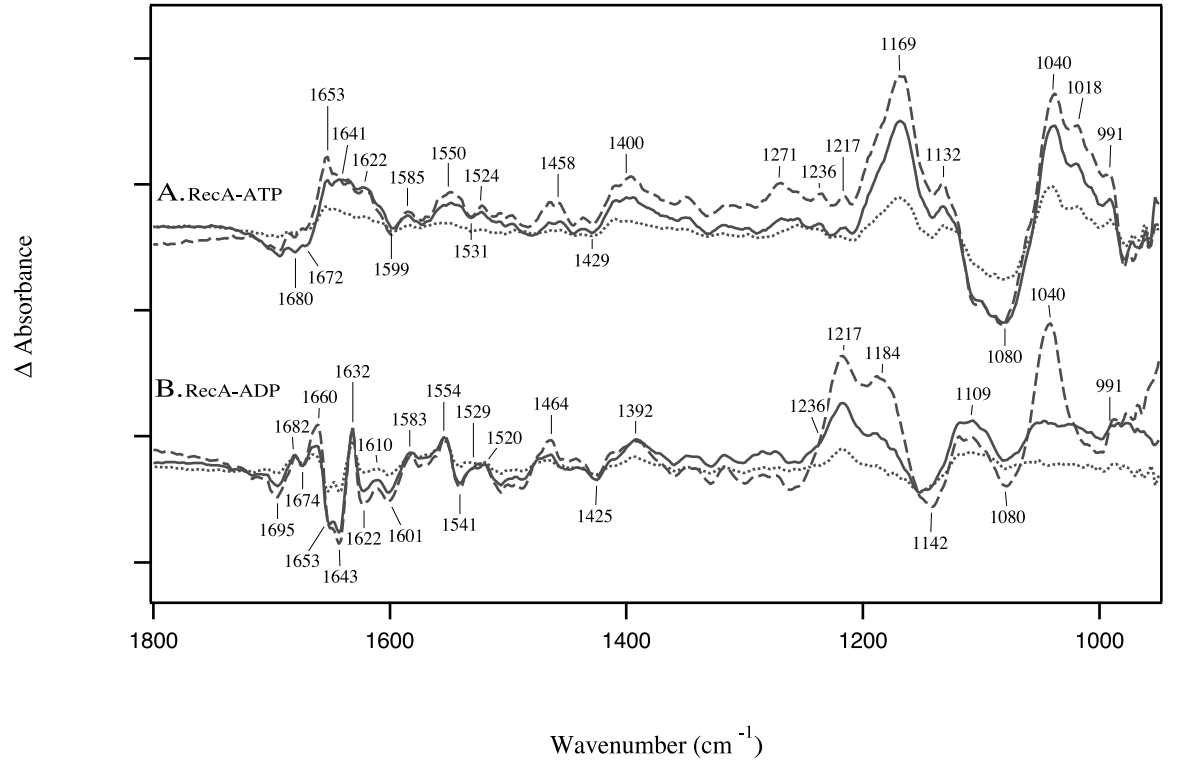

FIGURE 7 Data obtained using the data acquisition scheme shown in Fig. 6. The data presented was obtained on the same samples used to generate the data presented in Fig. 4 (*solid lines*). The difference spectra presented represent the difference spectra associated with subsequent light spectra ratioed against the first light taken immediately after photolysis. The difference data correspond to spectra taken 15 min (*dotted lines*), 60 min (*solid lines*), and ~110 min (*dashed lines*) after the first light spectrum. Fig. 7 *A* represents data obtained on samples containing RecA and caged ATP. Fig. 7 *B* represents difference data obtained samples containing RecA and caged ADP. The tick marks on the *y* axis correspond to 1×10^{-3} absorbance units.

nucleotides because all photolysis changes occur before the first light spectrum is obtained. Therefore, the spectra shown in Fig. 7 isolate changes that occur in the protein and/or nucleotide over time. However, it is possible that nucleotide-cage or cage-protein interactions that occur over time could contribute to the difference data, even though the subtraction artifacts have been eliminated. Dark minus dark spectra taken over extended time periods sometimes reveal very broad signals centered around 1650 and 1550 cm^{-1} that may arise from bench instability or temperature fluctuations. However, the spectra shown in Fig. 7 show unique vibrations when compared with the dark minus dark spectra described above. The largest differential signals present in Fig. 4 are at least four times the size of those observed in Fig. 7. The small changes observed in Fig. 7 suggest that the residual binding only affects a small amount of the protein and/or nucleotide present in the infrared samples. We speculate that the initial binding results in most of the redistribution of the RecA filaments, whereas subsequent protein-nucleotide interactions have more localized effects.

The data in Fig. 7 allow us to investigate changes that occur in the phosphate region below 1300 cm^{-1}. In the RecA-ATP data (Fig. 7 *A*) we observe a strong negative vibration around 1080 cm^{-1} and increases in the positive vibrations around 1169,1132, and the 1040–990 cm^{-1} region over time. Barth observed a positive vibrations around 1170 cm^{-1} and 1080 cm^{-1} and a negative 1230 cm^{-1} vibration in model spectra associated with ADP + P_i minus ATP (Barth et al., 1990). Although we observe a positive 1169 cm^{-1} vibration that increases over time, the negative 1230 and positive 1080 cm^{-1} vibrations may overlap or cancel with other changes associated with residual ATP binding or any other changes that may contribute to the spectra. The broad signal around 1080 cm^{-1} may correspond to $\nu_s(\beta-PO_2^-)$ of an ATP vibration that is perturbed upon binding to RecA (Takeuchi et al., 1988). The 991 cm^{-1} vibration that is present in the ATP spectrum does not increase over time in the ADP spectra (Fig. 7 *B*). Takeuchi has assigned a 990 cm^{-1} vibration to the ν(P−O) of the P_α-O-P_β linkage of ATP (Takeuchi et al., 1988). However, a 991 cm^{-1} vibration has also been previously assigned to symmetric stretching vibration of the (PO_3^{2-}) moiety in monohydrogen phosphate (Allin and Gerwert, 2001; Cepus et al., 1998b). Allin and Gerwert used $H_2{}^{18}O$ to assign the 1078 and 992 cm^{-1} vibrations to the formation of P_i that occurs in the GTPase, Ras (Allin and Gerwert, 2001). We are not able to definitively assign any of the vibrations observed at 1169, 1040, and 991 cm^{-1} to the formation of ADP and P_i. However, we have performed similar experiments under conditions (3.6 M KCl) where RecA would be expected to hydrolyze substantial amounts of ATP (Pugh and Cox, 1988). Under these high-salt conditions we observe enhanced positive vibrations around 1175, 1040, and 990 cm^{-1} that increase over time (data not shown). The conditions used in our experiments are not unique, studies performed on Ca^{2+}-ATPase have successfully followed ATP binding, and phosphorylation under hydration and temperature conditions very similar to those we have used (vonGermar et al., 2000). Furthermore, previous studies in our laboratory have shown that the dehydration procedure itself does not substantially alter RecA ATPase activity (Brewer et al., 2000). Therefore, in addition to contributions attributable to ATP binding, we can not rule out the possibility that a small amount of ATP hydrolysis may contribute to the spectra presented in Fig. 7 *A*. Future experiments will allow us to better identify the origin of the vibrations observed in Fig. 7.

The RecA-ATP spectra (Fig. 7 *A*) do not contain the sharp differential signals associated with residual ADP binding (Fig. 7 *B*). We speculate that the data presented in Fig. 7 *A* contain more heterogeneous changes in the protein and nucleotide. The initial spectra taken after only 15 min (Fig. 7 *A*, *dotted line*) shows small changes throughout the spectrum. However, at later times the broad changes around 1690–1620 cm^{-1} indicate that there may be various RecA-ATP states because of binding and/or hydrolysis of ATP. The solid line (Fig. 7 *A*) represents a ratio of data taken ~60 min after photolysis and contains negative contributions in the 1670–1680 cm^{-1} region. However, data taken approximately 110 min after release (Fig. 7 *A*, *dashed line*) show decreased negative intensity in the 1670–1680 cm^{-1} region concomitant with the increase in vibrations consistent with the formation of ADP + P_i or residual ATP interactions (Allin and Gerwert, 2001; Cepus et al., 1998b; Takeuchi et al., 1988). The ADP-RecA spectra in Fig. 7 *B* clearly show differential features in this region and a positive (rather than negative) vibration at 1680 cm^{-1} that is associated with ADP binding. Interestingly, the 1670–1680 cm^{-1} region of the RecA-ATP and RecA-ADP spectra could contain contributions from the nucleotide, protein secondary structural changes or amino acid side chains such as Gln, Arg, and Asn (Venyaminov and Kalnin, 1990b; Jackson and Mantsch, 1995).

The RecA-ATP data contain positive 1524 cm^{-1} vibrations and a negative vibration around 1530 cm^{-1} that are consistent with the involvement of Tyr and Lys side chains, respectively (Venyaminov and Kalnin, 1990b). There is a positive 1529 cm^{-1} vibration in the Rec-ADP data that may suggest different environments for a Lys side chain (Venyaminov and Kalnin, 1990b). This region may also include changes attributable to the secondary structure of the protein. However, the 1530 cm^{-1} region is of particular interest because the data in Fig. 4 may contain artifacts as a result of the subtraction of the photolysis contributions. Positive vibrations around 1585 cm^{-1} are now observed in both the ATP and ADP RecA spectra. The positive and negative vibrations present in the spectra shown in Fig. 7 *B* correlate extremely well with the changes observed in Fig. 4 *B*, suggesting that the data shown in Fig. 4 *B* do not contain substantial artifacts because of subtraction procedures. This

result is expected because the myoglobin-nucleotide data in Fig. 3 *C* contain only minimal changes in the 1800–1300 cm^{-1} region. However, the RecA-ADP data in Fig. 7 *B* spectra are missing the intense positive feature around 1645 cm^{-1} that present in the data in Fig. 4 *B*. Interestingly, the positive 1645 cm^{-1} vibration does seem to change over time and suggests that this vibration may arise from more substantial secondary structural changes that occur during initial ADP binding.

CONCLUSION

Difference infrared spectroscopy is a powerful technique that has been successfully used to study structural perturbations induced by nucleotide binding to RecA. Control experiments suggest that the caged nucleotides used in these experiments do not significantly interact with the RecA protein before photolytic release. Therefore, we can assume the difference spectra isolate protein and nucleotide changes that are induced upon nucleotide binding and do not contain vibrations associated with RecA-caged nucleotide interactions. Importantly, this technique allows us to study nucleotide-induced changes that occur throughout the entire wild-type protein. The difference infrared spectra reveal that nucleotide binding to RecA results in distinct secondary structural changes associated with allosteric regulation of RecA. Furthermore, the infrared data are consistent with previous studies that have suggested amino acids such as Asp, Glu, Lys, His, Arg, Gln, Asn, and Tyr help to modulate the affinity of RecA for DNA and the structure of the nucleoprotein filament.

The time-dependent data presented allow us to study vibrational changes in the absence of any subtraction artifacts and identify changes that occur in the phosphate region. The time-dependent data further substantiate the vibrations in the 1800–1300 cm^{-1} region are associated with ADP and ATP binding and are consistent with the possibility that RecA is able to hydrolyze ATP under the conditions used to generate difference infrared data presented here. Spectral features observed in the 1300–900 cm^{-1} of the time-dependent data confirm that the structure of the nucleotide phosphates are perturbed upon binding to RecA and provide us with a unique method of studying phosphate vibrations in the absence of subtraction artifacts. Future experiments will aid in determining whether the time-dependent changes observed in the RecA-ATP spectra are attributable to ATP binding, other nucleotide interactions, or if some of these changes may actually be associated with small amounts of ATP hydrolysis. Interestingly, the increase of vibrations that are associated with ATP interactions correlate with some changes in the 1670–1680 cm^{-1} region of the spectra. This observation, as well as the observed deuterium shifts in this region, support previous evidence suggesting crucial roles for Gln, Arg and Asn in cycling RecA between active and inactive conformations. Importantly, our experiments performed on the wild-type protein substantiate previous data obtained on RecA mutants and the L2 peptide (Voloshin et al., 2000). Unfortunately, the complexity of the spectral region of interest does not allow us to make definitive assignments of the vibrational changes observed. Although the spectra presented contain information that will lead to a detailed understanding of molecular changes induced by nucleotide binding, future studies are necessary to unambiguously resolve contributions from key amino acid side chains. The future studies will use global ^{15}N-labeling and the incorporation of isotopically labeled amino acids and/or nucleotides. These studies combined with the time-dependent infrared studies should result in a more complete description of the molecular changes crucial to the allosteric regulation of RecA.

This work was supported by NSF MCB-9733566 (to G.M.) and NSF-REU 97–31912.

REFERENCES

Allin, C., and K. Gerwert. 2001. Ras Catalyzes GTP hydrolysis by shifting negative charges from γ to β phosphate as revealed by time-resolved FTIR difference spectroscopy. *Biochemistry.* 40:3037–3046.

Barth, A., W. Kreutz, and W. Mantele. 1990. Molecular changes in the sarcoplasmic reticulum calcium ATPase during catalytic activity. A Fourier transform infrared (FTIR) study using photolysis of caged ATP to trigger the reaction cycle. *FEBS Lett.* 277:147–150.

Barth, A., W. Mantele, and W. Kreutz. 1991. Infrared spectroscopic signals arising from ligand binding and conformational changes in the catalytic cycle of sarcoplasmic reticulum calcium ATPase. *Biochim. Biophys. Acta.* 1057:115–123.

Bellamy, L. J. 1980. The Infrared Spectra of Complex Molecules. Chapman and Hall, London.

Brendel, V., L. Brocchieri, S. J. Sandler, A. J. Clark, and S. Karlin. 1997. Evolutionary comparisons of RecA-like proteins across all major kingdoms of living organisms. *J. Mol. Evol.* 44:528–541.

Brenner, S. L., A. Zlotnick, and J. D. Griffith. 1988. RecA protein self-assembly. Multiple discrete aggregation states. *J. Mol. Biol.* 204: 959–972.

Brenner, S. L., A. Zlotnick, and W. F. Stafford. III. 1990. RecA protein self-assembly II. Analytical equilibrium ultracentrifugation studies of the entropy-driven self-association of RecA. *J. Mol. Biol.* 216:949–964.

Brewer, S. H., S. G. Cresawn, D. T. Nguyen, and G. MacDonald. 2000. Difference FT-IR studies of nucleotide binding to the recombination protein RecA. *J. Phys. Chem. B.* 104:6950–6954.

Budzynski, D. M., X. Gao, and A. S. Benight. 1996. Isolation, characterization, and magnesium-induced self-association kinetics of discrete aggregates of RecA protein from *Escherichia coli. Biopolymers.* 38: 471–491.

Byler, D. M., and H. Susi. 1986. Examination of the secondary structure of proteins by deconvolved FTIR spectra. *Biopolymers.* 25:469–487.

Cepus, V., A. J. Scheidig, R. S. Goody, and K. Gerwert. 1998a. Time-resolved FTIR studies of the GTPase reaction of H-Ras P21 reveal a key role for the β-phosphate. *Biochemistry.* 37:10263–10271.

Cepus, V., C. Ulbrich, C. Allin, A. Troullier, and K. Gerwert. 1998b. Fourier transform infrared photolysis studies of caged compounds. *In* Methods in Enzymology. G. Marriott, editor. Academic Press, New York. 223–245.

Chirgadze, Y. N., O. V. Fedorov, and N. P. Trushina. 1975. Estimation of amino acid residue side-chain absorption in the infrared spectra of protein solutions in heavy water. *Biopolymers.* 14:679–694.

DeZutter, J. K., A. L. Forget, K. M. Logan, and K. L. Knight. 2001. Phe217 regulates the transfer of allosteric information across the subunit interface of the RecA protein filament. *Structure.* 9:47–55.

Dollinger, G., L. Eisenstein, S.-L. Lin, K. Nakanishi, and J. Termini. 1986. Fourier transform infrared difference spectroscopy of bacteriorhodopsin and its photoproducts regenerated with deuterated tyrosine. *Biochemistry.* 25:6524–6533.

Du, X., H. Frei, and S.-H. Kim. 2000. The mechanism of GTP hydrolysis by Ras probed by Fourier transform infrared spectroscopy. *J. Biol. Chem.* 275:8492–8500.

Egelman, E. H. 1993. What do X-ray crystallographic and electron microscopic structural studies of the RecA protein tell us about recombination? *Curr. Opin. Struct. Biol.* 3:189–197.

Eldin, S., A. L. Forget, D. M. Lindenmuth, K. M. Logan, and K. L. Knight. 2000. Mutations in the N-terminal region of RecA that disrupt the stability of free protein oligomers but not RecA-DNA complexes. *J. Mol. Biol.* 299:91–101.

Ellouze, C., M. Takahashi, P. Wittung, K. Mortensen, M. Schnarr, and B. Norden. 1995. Evidence for elongation of the helical pitch of the RecA filament upon ATP and ADP binding using small-angle neutron scattering. *Eur. J. Biochem.* 233:579–583.

El-Mahdaoui, L., and H. A. Tajmir-Riahi. 1995. A comparative study of ATP and GTP complexation with trivalent Al, Ga and Fe cations. Determination of cation binding site and nucleotide conformation by FTIR difference spectroscopy. *J. Biomol. Struct. Dyn.* 13:69–86.

Hortnagel, K., O. N. Voloshin, H. H. Kinal, N. M. Schaffer-Judge, and R. D. Camerini-Otero. 1999. Saturation mutagenesis of the *E. coli* RecA loop L2 homologous DNA pairing region reveals residues essential for recombination and recombinational repair. *J. Mol. Biol.* 286:1097–1106.

Jackson, M., and H. H. Mantsch. 1995. The use and misuse of FTIR spectroscopy in the determination of protein structure. *Crit. Rev. Biochem. Mol. Biol.* 30:95–120.

Kelley, J. A., and K. L. Knight. 1997. Allosteric regulation of RecA protein function is mediated by Gln194. *J. Biol. Chem.* 272:25778–25782.

Kim, S., J. Liang, and B. A. Barry. 1997. Chemical complementation identifies a proton acceptor for redox-active tyrosine D in photosystem II. *Proc. Natl. Acad. Sci. U.S.A.* 94:14406–14411.

Kim, S. K., B. Norden, and M. Takahashi. 1993. Role of DNA intercalators in the binding of RecA to double-stranded DNA. *J. Biol. Chem.* 268: 14799–14804.

Kowalczykowski, S. C., and R. A. Krupp. 1995. DNA-strand exchange promoted by RecA protein in the absence of ATP-Implications for the mechanism of energy transduction in protein-promoted nucleic acid transactions. *Proc. Natl. Acad. Sci. U.S.A.* 92:3478–3482.

Lee, J. W., and M. M. Cox. 1990. Inhibition of RecA protein promoted ATP hydrolysis. 1. ATPγS and ADP are antagonistic inhibitors. *Biochemistry.* 29:7666–7676.

Menetski, J. P., and S. C. Kowalczykowski. 1985. Interaction of recA protein with single-stranded DNA. Quantitative aspects of binding affinity modulation by nucleotide cofactors. *J. Mol. Biol.* 181:281–295.

Mikawa, T., R. Masui, and S. Kuramitsu. 1998. RecA protein has extremely high cooperativity for substrate in its ATPase activity. *J. Biochem.* 123:450–457.

Morimatsu, K., T. Horii, and M. Takahashi. 1995. Interaction of Tyr103 and Tyr264 of the RecA protein with DNA and nucleotide cofactors. Fluorescence study of engineered proteins. *Eur. J. Biochem.* 228: 779–785.

Pugh, B. F., and M. M. Cox. 1988. High salt activation of recA protein ATPase in the absence of DNA. *J. Biol. Chem.* 263:76–83.

Raimbault, C., F. Besson, and R. Buchet. 1997. Conformational changes of arginine kinase induced by photochemical release of nucleotides from caged nucleotides. An infrared difference-spectroscopy investigation. *Eur. J. Biochem.* 244:343–351.

Rehrauer, W. M., and S. C. Kowalczykowski. 1993. Alteration of the nucleoside triphosphate (NTP) catalytic domain within *E. coli* RecA protein attenuates NTP hydrolysis but not joint molecule formation. *J. Biol. Chem.* 268:1292–1297.

Roca, A. I., and M. M. Cox. 1990. The RecA protein: structure and function. *Crit. Rev. Biochem. Mol. Biol.* 25:415–456.

Roca, A. I., and M. M. Cox. 1997. RecA protein: structure, function, and role in recombinational DNA repair. *In* Progress in Nucleic Acid Research and Molecular Biology, Vol. 56. Cohn and K. Moldave, editors. Academic Press, San Diego.129–223.

Shan, Q., M. M. Cox, and R. B. Inman. 1996. DNA strand exchange promoted by RecA K72R. *J. Biol. Chem.* 271:5712–5724.

Stole, E., and F. R. Bryant. 1996. Reengineering the nucleotide cofactor specificity of the RecA protein by mutation of aspartic acid 100*-. *J. Biol. Chem.* 271:18326–18328.

Stole, E., and F. R. Bryant. 1994. Introduction of a tryptophan reporter group into loop 1 of the RecA protein. *J. Biol. Chem.* 269:7919–7925.

Story, R. M., and T. A. Steitz. 1992. Structure of the RecA protein-ADP complex. *Nature.* 355:374–376.

Story, R. M., I. T. Weber, and T. A. Steitz. 1992. The structure of the *E. coli* RecA protein monomer and polymer. *Nature.* 355:318–325.

Takahashi, M., F. Maraboeuf, and B. Norden. 1996. Locations of functional domains in the RecA protein. Overlap of domains and regulation of activities. *Eur. J. Biochem.* 242:20–28.

Takeuchi, H., H. Murata, and Harada, I. 1988. Interaction of adenosine 5′-triphosphate with Mg^{2+}: vibrational study of coordination sites by use of ^{18}O-labeled triphosphates. *J. Am. Chem. Soc.* 110:392–397.

Venyaminov, S. Y., and N. N. Kalnin. 1990a. Quantitative IR spectrophotometry of peptide compounds in water (H_2O) solutions. II. Amide absorption bands of polypeptides and fibrous proteins in α-,β-, and random coil conformations. *Biopolymers.* 30:1259–1271.

Venyaminov, S. Y., and N. N. Kalnin. 1990b. Quantitative IR spectrophotometry of peptide compounds in water (H_2O) solutions. I. Spectral parameters of amino acid residue absorption bands. *Biopolymers.* 30: 1243–1257.

Voloshin, O. N., L. Wang, and R. D. Camerini-Otero. 2000. The homologous pairing domain of RecA also mediates the allosteric regulation of DNA binding and ATP hydrolysis: a remarkable concentration of functional residues. *J. Mol. Biol.* 303:709–720.

von Germar, F., A. Barth, and W. Mantele. 2000. Structural changes of the sarcoplasmic reticulum Ca^{2+}-ATPase upon nucleotide binding studied by Fourier transform infrared spectroscopy. *Biophys. J.* 78:1531–1540.

von Germar, F., A. Galan, O. Llorca, J. L. Carrascosa, J. M. Valpuesta, W. Mantele, and A. Muga. 1999. Conformational changes generated in GroEL during ATP hydrolysis as seen by time-resolved infrared spectroscopy. *J. Biol. Chem.* 274:5508–5513.

Wittung, P., B. Norden, and M. Takahashi. 1995. Secondary structure of RecA in solution. The effects of cofactor, DNA and ionic conditions. *Eur. J. Biochem.* 228:149–154.

Yu, X., and E. H. Egelman. 1992. Structural data suggest that the active and inactive forms of the RecA filament are not simply interconvertible. *J. Mol. Biol.* 227:334–346.